Hermite interpolation by planar cubic-like ATPH

Thierry Bay, Isabelle Cattiaux-Huillard, Laura Saini

Hermite interpolation by planar cubic-like ATPH

Thierry Bay[1], Isabelle Cattiaux-Huillard[1], and Laura Saini[2]

[1]Université Polytechnique Hauts-de-France, CERAMATHS, FR CNRS 2037, F-59313 Valenciennes, France - thierry.bay@uphf.fr, isabelle.cattiaux@uphf.fr
[2]Junia, Computer Science and Mathematics, F-59000 Lille, France - laura.saini@junia.com

February 4, 2022

Abstract

This paper deals with the construction of the Algebraic Trigonometric Pythagorean Hodograph (ATPH) cubic Hermite interpolant and analyzes the existence and characterizations of solutions according to the tangents at both ends and a global shape parameter denoted α. Since this degree of freedom can be used for adjustments, we study how the curve evolves with respect to α. As an example of the use of this parameter, a simple fitting method is proposed to determine the unique ATPH curve passing through a given point in addition to the Hermite constraints.

Keywords: Pythagorean hodograph · Trigonometric functions · Algebraic trigonometric · Trigonometric polynomials · Circle arc · Hermite interpolation

Mathematics Subject Classifications (2020): 41A05 · 42A15 · 51N05 · 65D05 · 65D07 · 65D10 · 65D17 · 68U07

1 Introduction

The most commonly used schemes in CAD and CAGD for the representation of curves and surfaces are specified by polynomial and rational parameterizations, such as Bézier curves, B-splines or NURBS. Even though these models offer many advantages, they have important drawbacks that Mainar et al. detailed in [6]. For example, on the one hand, calculations related to polynomial parameterization are quite simple but only make it possible to represent a restricted range of curves, excluding conics. On the other hand, rational parameterization allows us to obtain conics and trigonometric curves, but comes at the expense of additional weights for each control point or a less user-friendly process for differentiation. To avoid these inconveniences, it could be interesting to investigate other curve spaces.

In order to generalize the Bernstein bases (while preserving their most important properties) for other function spaces, Carnicer and Peña have introduced in [2] the concept of B-basis. Mainar et al. have provided in [6] criteria for finding a B-basis in a general case. The curves they defined display all the positive properties of the Bézier scheme from variation diminishing to tangency to the control polygon at the endpoints. The reader can refer to their work for further details.

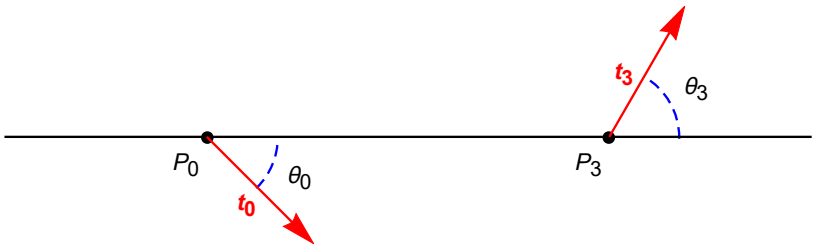

Figure 1: G^1 Hermite interpolation data.

The authors in [6] gave a particular solution for the mixed Algebraic Trigonometric curve (AT curve thereafter) space $\mathcal{P}_m(\mathbb{K}) = span\{1, t, \{\cos(kt), \sin(kt)\}_{k=1}^{m}\}$ for $m = 1$ and $m = 2$ (where $\mathbb{K}$ can be either $\mathbb{R}$ or $\mathbb{C}$). They defined in this paper a B-basis $\{Z_k(t)\}_{k=0}^{3}$ of the cycloidal curve space $\mathcal{P}_1(\mathbb{K})$, described on $[0, \alpha]$ with $\alpha \in]0, 2\pi[$ a global shape parameter. A Wolfram demonstration of these bases and curves is available in [3].

The underlying benefits of the previously cited mixed AT space $P_m(\mathbb{K})$ has then been combined with the Pythagorean Hodograph (PH) feature in [9]. Indeed, PH curves, introduced by Farouki and Sakkalis in [5] for the Bézier curves, enable to compute explicitly the arc length, the curvature, or the offset curves. A new class of curves, denoted ATPH, was partially investigated in [9] for $m = 2$. In [4], the authors gave a straightforward and exhaustive description of these curves through their complex expression, and proposed an in-depth study of spaces $\mathcal{P}_1(\mathbb{K})$ and $\mathcal{P}_2(\mathbb{K})$.

In particular, ATPH curves have degrees of freedom which could be used in different areas such as interpolation problems. In this paper, we will investigate ATPH in $\mathcal{P}_1(\mathbb{R})$ to find the geometric Hermite interpolant.

In Section 2, we start with the study of the construction of cubic ATPH Hermite interpolants. Then, we analyze in Section 3 the conditions needed for the existence of such solutions. As we will see throughout this paper, the ATPH solutions depend on the α parameter which can be used for solving other problems. Consequently in Section 4, we look at the influence of α on the curve shape by working on the control polygon. Finally, in Section 5 we focus on an example showing how to find the ATPH cubic Hermite interpolant that passes through one given additional point.

2 A cubic ATPH for the Hermite problem

The Hermite problem we are going to deal with consists of interpolating two points and two tangent directions by a cubic ATPH curve. Therefore, we consider two distinct points $\mathbf{P}_0$ and $\mathbf{P}_3$ and two oriented angles, $\theta_0 \in [-\pi, 0]$ and $\theta_3 \in [0, 2\pi[$. The choice of these intervals allows us to study all possible cases without any loss of generality.

In the coordinate system $(\mathbf{P}_0, \mathbf{i}, \mathbf{j})$ where $\mathbf{i} = \dfrac{\mathbf{P}_3 - \mathbf{P}_0}{\|\mathbf{P}_3 - \mathbf{P}_0\|}$ and $\mathbf{j} = \mathrm{rot}_{\frac{\pi}{2}}(\mathbf{i})$, we define two unit tangent vectors $\mathbf{t}_0 = (\cos\theta_0, \sin\theta_0)$ and $\mathbf{t}_3 = (\cos\theta_3, \sin\theta_3)$ (cf. Figure 1).

Let $\mathbf{r}_\alpha(t)$ be the parameterization of the solution for a given value of α belonging to $]0, 2\pi[$

and $\mathbf{P} = (\mathbf{P}_0, \mathbf{P}_1, \mathbf{P}_2, \mathbf{P}_3)$ its control polygon relative to the B-basis. We need to verify:

$$\begin{aligned} \mathbf{r}_\alpha(0) &= \mathbf{P}_0, & \mathbf{r}_\alpha(\alpha) &= \mathbf{P}_3, \\ \frac{d\mathbf{r}_\alpha}{dt}(0) &= \lambda_0 \mathbf{t}_0, & \frac{d\mathbf{r}_\alpha}{dt}(\alpha) &= \lambda_3 \mathbf{t}_3, \end{aligned}$$

where λ_0 and λ_3 are strictly positive real numbers. Note that if $\mathbf{t}_0$ and $\mathbf{t}_3$ are both collinear with $\mathbf{P}_3 - \mathbf{P}_0$, the solution of Hermite's problem is trivially a line segment and is of little interest. Therefore, we will exclude this case in the rest of the article, and we will denote by $\mathcal{H}$ the domain $[-\pi, 0] \times [0, 2\pi[$ for (θ_0, θ_3) without couples $(-\pi, 0)$, $(-\pi, \pi)$, $(0, 0)$ and $(0, \pi)$.

According to [4], a cubic ATPH curve is characterized by the complex relation:

$$(\Delta \mathbf{p}_1)^2 = K_\alpha \Delta \mathbf{p}_0 \Delta \mathbf{p}_2 \qquad \text{with} \qquad K_\alpha = \frac{4}{(\alpha - \sin\alpha)^2} \left(2 \sin\frac{\alpha}{2} - \alpha \cos\frac{\alpha}{2}\right)^2, \tag{1}$$

where $\mathbf{p}_i$ is the complex form of the control point $\mathbf{P}_i$ for $i = 0, 1, 2, 3$. From these expressions we get:

$$l_1^2 = K_\alpha l_0 l_2 \qquad \text{and} \qquad \theta_1 = \theta_2, \tag{2}$$

where $\theta_1 = \angle(\mathbf{P}_0 - \mathbf{P}_1, \mathbf{P}_2 - \mathbf{P}_1)$, $\theta_2 = \angle(\mathbf{P}_1 - \mathbf{P}_2, \mathbf{P}_3 - \mathbf{P}_2)$ and, in polar form, $\Delta \mathbf{p}_k = \mathbf{p}_{k+1} - \mathbf{p}_k = l_k e^{i\beta_k}$ for $k = 0, 1, 2$ (cf. Figure 2).

In the sequel, the K_α value appears many times. It is therefore necessary to detail its elementary properties that can be established by some straightforward calculations.

Proposition 1. *The term K_α is an increasing and continuous function of α. It belongs to the range $]1, 4]$ when α is in the interval $]0, 2\pi]$ and K_α tends to 1 as α approaches 0. Moreover*

$$\sqrt{K_\alpha} = \frac{2}{\alpha - \sin\alpha} \left(2 \sin\frac{\alpha}{2} - \alpha \cos\frac{\alpha}{2}\right).$$

From the data described above, we have $\theta_1 = \pi - \beta_0 + \beta_1$ and $\theta_2 = \pi - \beta_1 + \beta_2$. Besides, the Hermite conditions G^1 imply $\beta_0 = \theta_0$ and $\beta_2 = \theta_3$. From (2), we therefore deduce $-\beta_0 + \beta_1 = -\beta_1 + \beta_2$, hence $\beta_1 = \frac{1}{2}(\beta_0 + \beta_2)$ to within π. So

$$\beta_1 = \frac{1}{2}(\theta_0 + \theta_3) \qquad \text{or} \qquad \beta_1 = \frac{1}{2}(\theta_0 + \theta_3) + \pi. \tag{3}$$

To begin with, let us consider the first possibility. We will see afterwards how to take into account the second one.

By Chasles' relation, we obtain:

$$\begin{aligned} \Delta \mathbf{p}_0 + \Delta \mathbf{p}_1 + \Delta \mathbf{p}_2 &= \mathbf{p}_3 - \mathbf{p}_0, \\ l_0 e^{i\beta_0} + l_1 e^{i\beta_1} + l_2 e^{i\beta_2} &= \mathbf{p}_3 - \mathbf{p}_0, \\ l_0 e^{i\theta_0} + \sqrt{K_\alpha l_0 l_2}\; e^{i\frac{\theta_0+\theta_3}{2}} + l_2 e^{i\theta_3} &= \mathbf{p}_3 - \mathbf{p}_0, \end{aligned} \tag{4}$$

so, if we set $L = \sqrt{\dfrac{l_2}{l_0}}$:

$$(3) \;\Leftrightarrow\; e^{i\theta_0} + L\sqrt{K_\alpha}\; e^{i\frac{\theta_0+\theta_3}{2}} + L^2 e^{i\theta_3} = \frac{\mathbf{p}_3 - \mathbf{p}_0}{l_0}, \tag{5}$$

$$\Im m(5) \;\Leftrightarrow\; \sin\theta_0 + L\sqrt{K_\alpha} \sin\left(\frac{\theta_0 + \theta_3}{2}\right) + L^2 \sin\theta_3 = 0, \tag{6}$$

$$\Re e(5) \;\Leftrightarrow\; \cos\theta_0 + L\sqrt{K_\alpha} \cos\left(\frac{\theta_0 + \theta_3}{2}\right) + L^2 \cos\theta_3 = \frac{\|\mathbf{P}_3 - \mathbf{P}_0\|}{l_0}. \tag{7}$$

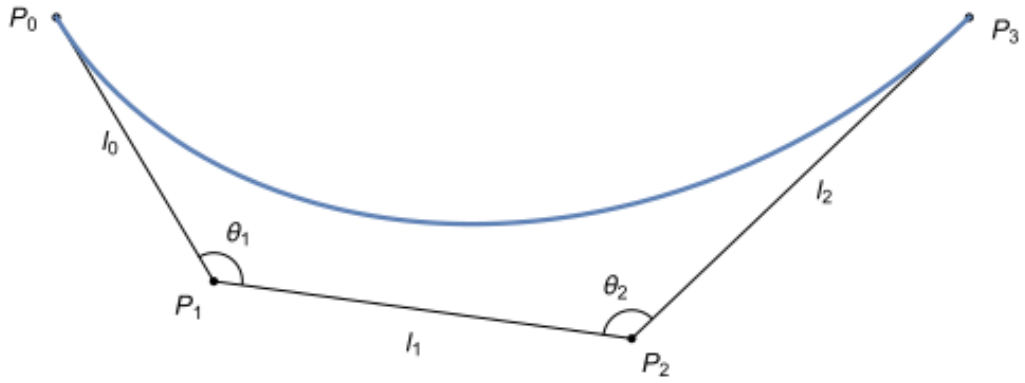

Figure 2: Cubic ATPH polygon data.

When the degree of equation (6) is 2, i.e. for $\theta_3 \neq 0$ and $\theta_3 \neq \pi$, the discriminant is

$$\Delta = K_\alpha \sin^2\left(\frac{\theta_0+\theta_3}{2}\right) - 4\sin\theta_0 \sin\theta_3, \tag{8}$$

and the solutions, when they exist, are

$$L_\varepsilon = \frac{1}{2\sin\theta_3}\left(-\sqrt{K_\alpha}\sin\left(\frac{\theta_0+\theta_3}{2}\right) + \varepsilon\sqrt{\Delta}\right), \tag{9}$$

where $\varepsilon \in \{-1,+1\}$. For the sake of clarity, we will denote them respectively L_- and L_+. When the real number

$$G_\varepsilon = \cos\theta_0 + L_\varepsilon\sqrt{K_\alpha}\cos\left(\frac{\theta_0+\theta_3}{2}\right) + L_\varepsilon^2\cos\theta_3, \tag{10}$$

is positive, we deduce from (7) the value of l_0 and then l_2. With the previous expressions of β_0, β_1 and β_2, we can determine $\Delta\mathbf{p}_i$, for $i = 0, 1, 2$ and therefore the control polygon of the solution $\mathbf{r}_\alpha$.

When $\theta_3 = 0$ or $\theta_3 = \pi$, equation (6) is of degree 1 and requires a specific study which is done in Section 3.4.

Remark 1. *The values $\alpha = 0$ and $\alpha = 2\pi$ are excluded from the study. On one hand, the second and third functions $Z_1(t)$ and $Z_2(t)$ of the B-basis become null as α approaches 2π. Therefore $\mathbf{r}_\alpha$ tends to the segment $[\mathbf{P}_0\mathbf{P}_3]$, which obviously constitutes an improper solution (it will however be useful in the last part of this article). On the other hand, when α approaches 0, the cubic AT curve becomes the cubic polynomial Bézier curve of the same control polygon as shown by Zhang in [11]. This is consistent with the results of this part, since when the parameter K_α tends to 1, the expressions (8), (9) and (10) are identical to the formula given by Walton and Meek in [7] and by Byrtus and Bastl in [1] for the polynomial case.*

3 Existence of solutions

The solutions described in the previous part do not always exist. We now have to clarify their conditions of existence, i.e. the domains on which the values of Δ, G_ε, L_ε, defined by the

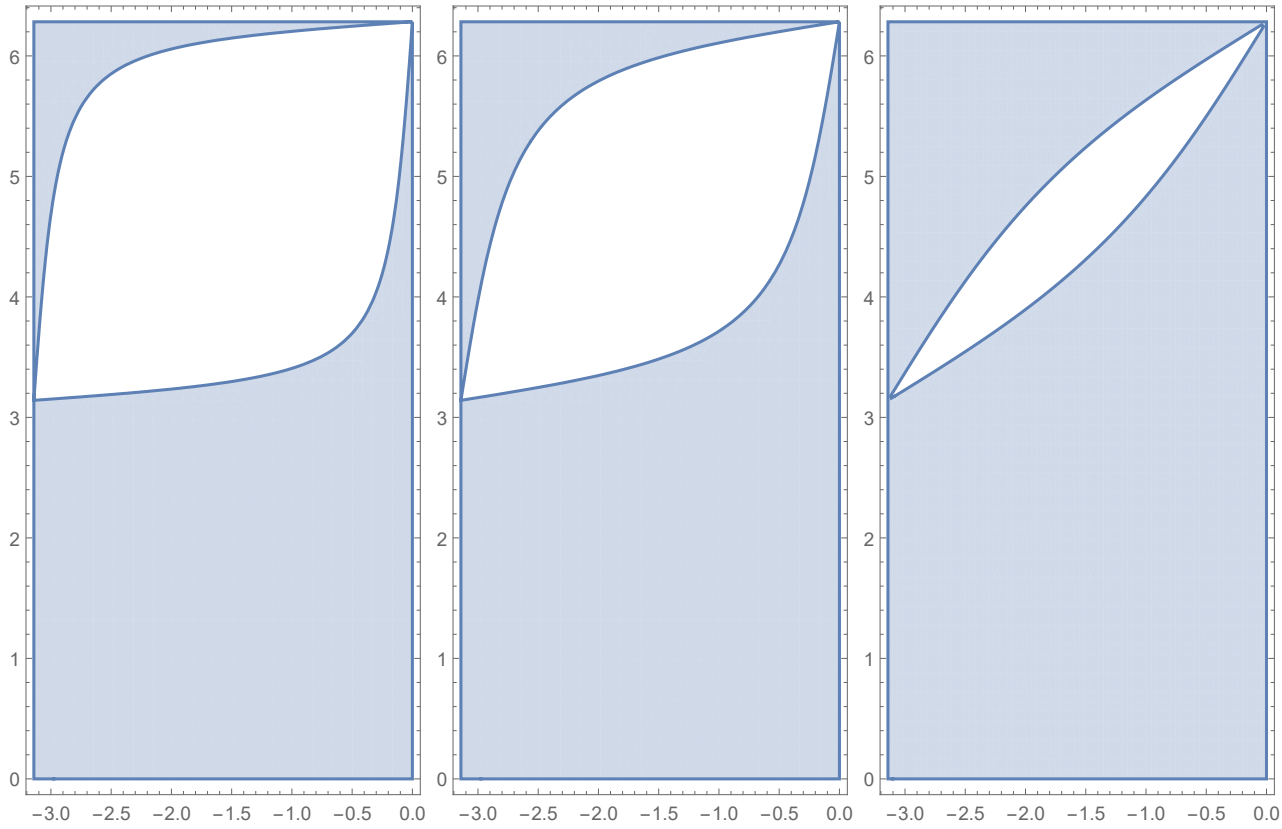

Figure 3: Domain $\mathcal{D}_+$ for $\alpha = \dfrac{\pi}{6}$, $\alpha = \dfrac{7\pi}{6}$ and $\alpha = \dfrac{11\pi}{6}$.

expressions (8), (9), (10) are positive. As said previously, the cases $\theta_3 = 0$ and $\theta_3 = \pi$ are different from the general one and will be treated separately.

3.1 Sign of the discriminant

Let us denote by $\mathcal{D}_+$ the domain of $\mathcal{H}$ where $\Delta \geq 0$, whose boundary is defined by the functions:

$$f_1(\theta_0) = 2\pi - \arccos \frac{K_\alpha^2 \cos\theta_0 - 4(8-K_\alpha)\sqrt{4-K_\alpha}\sin^2\theta_0}{K_\alpha^2 + 16(4-K_\alpha)\sin^2\theta_0},$$

$$f_2(\theta_0) = 2\pi - \arccos \frac{K_\alpha^2 \cos\theta_0 + 4(8-K_\alpha)\sqrt{4-K_\alpha}\sin^2\theta_0}{K_\alpha^2 + 16(4-K_\alpha)\sin^2\theta_0}.$$

Since $K_\alpha \in]1,4[$, these two functions are well defined for any value of $\alpha \in]0, 2\pi[$. Of course, the shape of this domain depends on this last parameter (see Figure 3). The function f_1 describes the lower border of the domain, and f_2 the upper border (see Figure 4). So the domain $\mathcal{D}_+$ is described by

$$\mathcal{D}_+ = \{(\theta_0, \theta_3) \in \mathcal{H} \mid \theta_3 \leq f_1(\theta_0) \text{ or } f_2(\theta_0) \leq \theta_3\}.$$

We can remark that for $\theta_3 < \pi$, we have $\Delta > 0$, hence the condition is always verified.

3.2 Sign of l_0

Once L_ε is determined using (9), l_0 is obtained from the relation (7). Therefore, l_0 and the real number G_ε have the same sign which has to be positive. Moreover, the case $G_\varepsilon = 0$ should

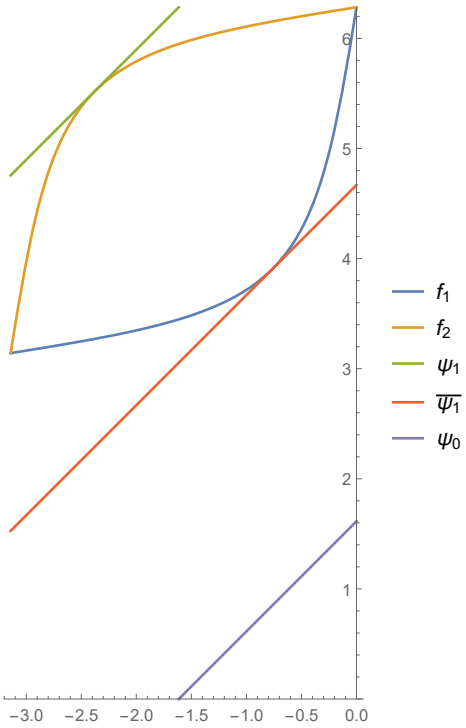

Figure 4: Edges of $\mathcal{D}_+$, Γ_+ and Γ_- domains for $\alpha = \dfrac{7\pi}{6}$.

be excluded, otherwise the length l_0 would be infinite. Here we will study the sign of G_ε, as defined in (10), using the expression (9) for L_ε.

Denoting Γ_+ and Γ_- the subdomains of $\mathcal{H}$ where $G_+ > 0$ and $G_- > 0$ respectively, a solution exists if and only if (θ_0, θ_3) belongs to $\Gamma = \Gamma_+ \cup \Gamma_-$. The relations (9) and (10) allow us to establish, after some long calculations, that

$$\begin{aligned}
\Gamma_+ &= \{(\theta_0,\theta_3) \in \mathcal{H} \mid \theta_3 \geq \pi - \theta_0 \text{ and } (f_2(\theta_0) < \theta_3 < \psi_1(\theta_0) \text{ or } \theta_3 < f_1(\theta_0))\} \\
&\quad \cup \{(\theta_0,\theta_3) \in \mathcal{H} \mid \theta_3 < \pi - \theta_0 \text{ and } (\theta_3 < \overline{\psi_1}(\theta_0)\}, \\
\Gamma_- &= \{(\theta_0,\theta_3) \in \mathcal{H} \mid \theta_3 \geq \pi - \theta_0 \text{ and } (f_2(\theta_0) < \theta_3 \text{ or } \overline{\psi_1}(\theta_0) < \theta_3 < f_1(\theta_0))\} \\
&\quad \cup \{(\theta_0,\theta_3) \in \mathcal{H} \mid \theta_3 < \pi - \theta_0 \text{ and } (\theta_3 < \psi_0(\theta_0) \text{ or } \psi_1(\theta_0) < \theta_3)\},
\end{aligned}$$

with

$$\psi_k(\theta_0) = \theta_0 + \arccos\left(\frac{K_\alpha}{2} - 1\right) + 2k\pi, \tag{11}$$

$$\overline{\psi_k}(\theta_0) = \theta_0 - \arccos\left(\frac{K_\alpha}{2} - 1\right) + 2k\pi. \tag{12}$$

Since $K_\alpha \in]1, 4]$ according to Proposition 1, these functions are well defined. Only the lines corresponding to $\psi_0(\theta_0)$, $\psi_1(\theta_0)$ and $\overline{\psi_1}(\theta_0)$ are in the domain $\mathcal{H}$ (cf. Figure 4) and are involved in the description of Γ_+ and Γ_- (cf. Figures 5 and 6).

This result is a generalization of [1] focusing on the polynomial curves, which corresponds to the case $K_\alpha = 1$ for $\alpha = 0$ in our study. The ATPH feature provides therefore a wider domain of solutions through the variations induced by the α parameter.

Remark 2. *If $\Delta \geq 0$ and $G_\varepsilon < 0$, the curve exists with $l_0 < 0$ and therefore $l_2 < 0$. A length being positive, the notion of algebraic measure would then be more appropriate to cover this case.*

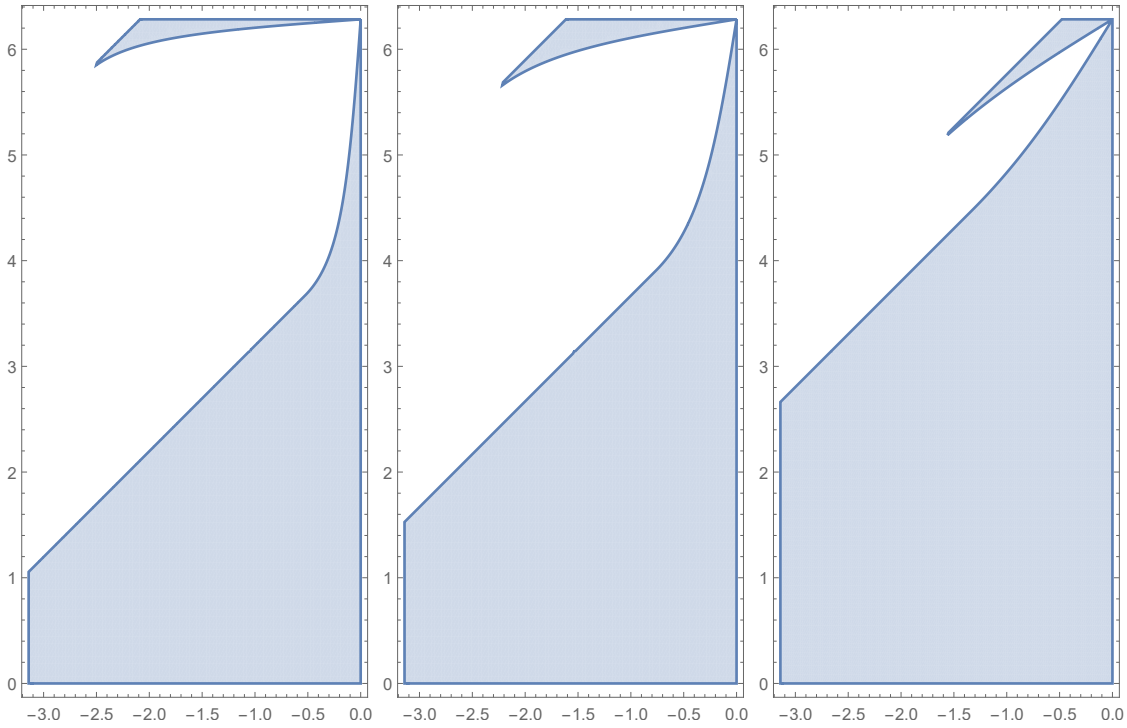

Figure 5: Subdomain Γ_+ for $\alpha = \dfrac{\pi}{6}$, $\alpha = \dfrac{7\pi}{6}$ and $\alpha = \dfrac{11\pi}{6}$.

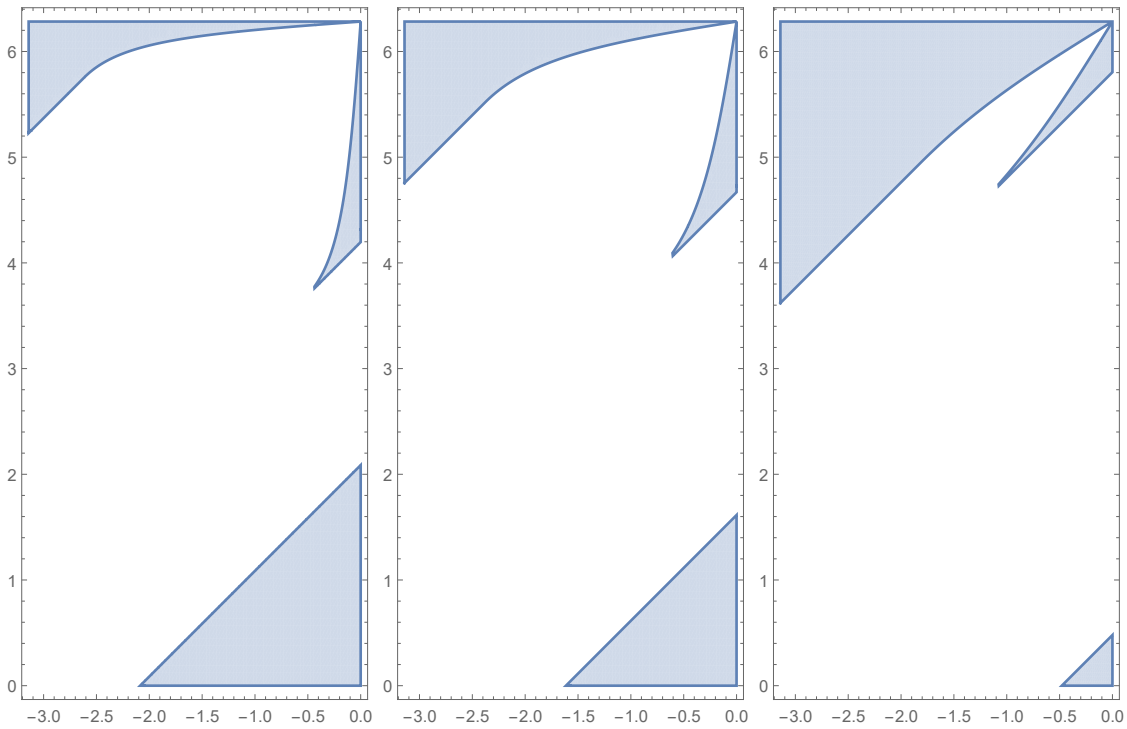

Figure 6: Subdomain Γ_- for $\alpha = \dfrac{\pi}{6}$, $\alpha = \dfrac{7\pi}{6}$ and $\alpha = \dfrac{11\pi}{6}$.

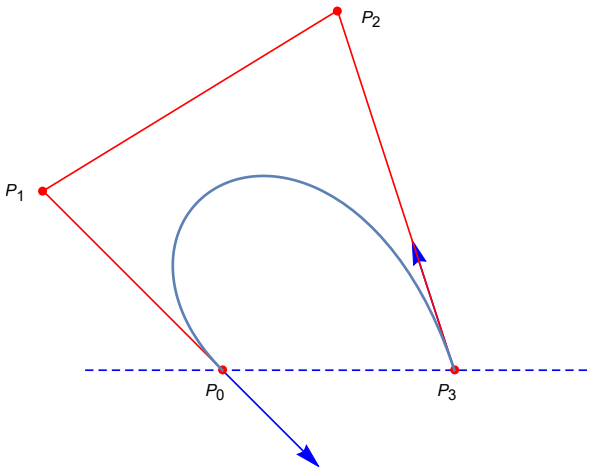

Figure 7: Improper solution when G_ε is negative, for $\alpha = \dfrac{2\pi}{3}$, $\theta_0 = -\dfrac{\pi}{4}$ and $\theta_0 = \dfrac{3\pi}{5}$.

As seen in Figure 7, this means geometrically that the orientations of $\overrightarrow{\mathbf{P}_0\mathbf{P}_1}$ *and* $\mathbf{t}_0$ *are opposite, as the orientations of* $\overrightarrow{\mathbf{P}_2\mathbf{P}_3}$ *and* $\mathbf{t}_3$ *are. If the constraints of the Hermite problem concern only the direction of the tangents and not their orientation, these solutions are convenient. The only condition that* θ_0 *and* θ_3 *must then verify is* $\Delta \geq 0$*, ie* $(\theta_0, \theta_3) \in \mathcal{D}_+$.

3.3 Sign of roots

As $L_\varepsilon = \sqrt{l_2/l_0}$, its value is positive. However, equation (6) can have negative roots. We will show that they are also solutions of the Hermite problem.

Relation (3) gives two expressions for β_1. The second one leads to slightly different expressions of equations (6) and (7):

$$\sin\theta_0 - L\sqrt{K_\alpha}\sin\left(\frac{\theta_0+\theta_3}{2}\right) + L^2\sin\theta_3 = 0, \tag{13}$$

$$\cos\theta_0 - L\sqrt{K_\alpha}\cos\left(\frac{\theta_0+\theta_3}{2}\right) + L^2\cos\theta_3 = \frac{\|\mathbf{P}_3-\mathbf{P}_0\|}{l_0}. \tag{14}$$

We notice that L_ε is a solution of (6) if and only if $-L_\varepsilon$ is a solution of (13). Therefore, the expression (14) with the solution $-L_\varepsilon$ of (13) is identical to the expression given by (7) for L_ε. So the value of l_0 is the same in both cases.

Proposition 2. *When* $L_\varepsilon < 0$*, we always have* $l_0 = \dfrac{\|\mathbf{P}_3-\mathbf{P}_0\|}{G_\varepsilon}$ *and* $l_2 = L_\varepsilon^2 l_0$*. In this case,* $\beta_1 = \pi + \dfrac{\theta_0+\theta_3}{2}$ *and the polygon* $(\mathbf{P}_0, \mathbf{P}_1, \mathbf{P}_2, \mathbf{P}_3)$ *is then crossed (see Figure 8).*

A crossed polygon often gives a looped curve, which is often unsuitable in CAGD. As a consequence, it is important to determine the sign of L_ε when $G_\varepsilon > 0$ and $\Delta \geq 0$. Some considerations about the roots of equation (6) lead to the following result.

Proposition 3. *When the roots of equation* (6) *exist and verify* $G_\varepsilon > 0$*, we have* $L_+ > 0$ *for all the values of* θ_0 *and* θ_3*, and* $L_- > 0$ *if and only if* $\theta_3 > \pi$*. The polygon is then crossed if and only if* $\varepsilon = -1$ *and* $\theta_3 < \pi$.

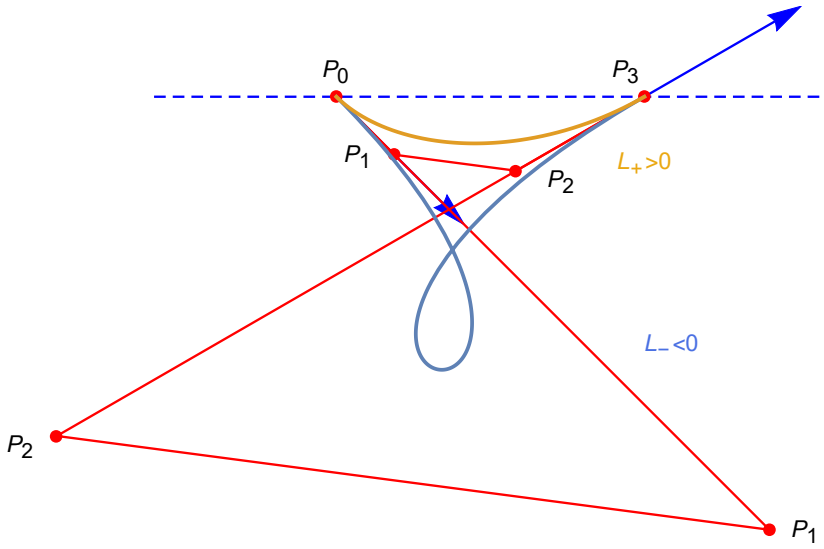

Figure 8: Example of a double solution with $L_+ > 0$ and $L_- < 0$.

3.4 Particular case: $\theta_3 = 0$ and $\theta_3 = \pi$

As said in Section 2, equation (6) is of degree 1 when $\theta_3 = 0$ or $\theta_3 = \pi$.

If $\theta_3 = 0$, its solution is then $L = L_0 = \dfrac{-2}{\sqrt{K_\alpha}} \cos\dfrac{\theta_0}{2}$ which is always negative. So $\beta_1 = \pi + \dfrac{\theta_0 + \theta_3}{2}$ (according to Proposition 2) and its polygon is Z-shaped. Denoting G_0 the equivalent of G_ε for L_0, we obtain from (14) $G_0 = 1 + \dfrac{2}{K_\alpha} + 2\left(1 + \dfrac{1}{K_\alpha}\right)\cos\theta_0$ which is positive if and only if $\theta_0 > \arccos\left(\dfrac{K_\alpha + 2}{2(K_\alpha + 1)}\right) - \pi$.

If $\theta_3 = \pi$, the solution of equation (6) is $L = L_\pi = \dfrac{-2}{\sqrt{K_\alpha}} \sin\dfrac{\theta_0}{2}$ which is positive. With the same convention, $G_\pi = \dfrac{1}{K_\alpha}(2\cos\theta_0 - 2 + K_\alpha)$ is positive if and only if $\theta_0 > -\arccos\left(1 - \dfrac{K_\alpha}{2}\right)$.

4 Evolution of l_0 and l_2 with respect to α

The shape of the control polygon determines the curve and may sometimes involve the presence of inflection points, cusps or loops. These elements are undesirable for most CAD, CAD/CAM, or computer graphics applications. In an upcoming paper, we will propose a characterization of the shape of an AT cubic curve according to its control polygon. For now, we will just assume that the control polygon is convex, which is a sufficient condition to eliminate undesired elements according to the variation diminishing property. Obviously, this requirement is equivalent to $\theta_3 < \pi$ and $\varepsilon = 1$. The corresponding two cases are illustrated in Figure 9.

The ATPH solution of the Hermite problem depends on α which gives an additional degree of freedom, the polynomial solution being a particular case obtained for $\alpha = 0$. This free parameter can be used to solve various additional problems (velocity, interpolation point, ...), as will be shown in Section 5. It is therefore important to analyze the evolution of the curve with respect to α. For this purpose, we will study a geometrical version of our problem throughout

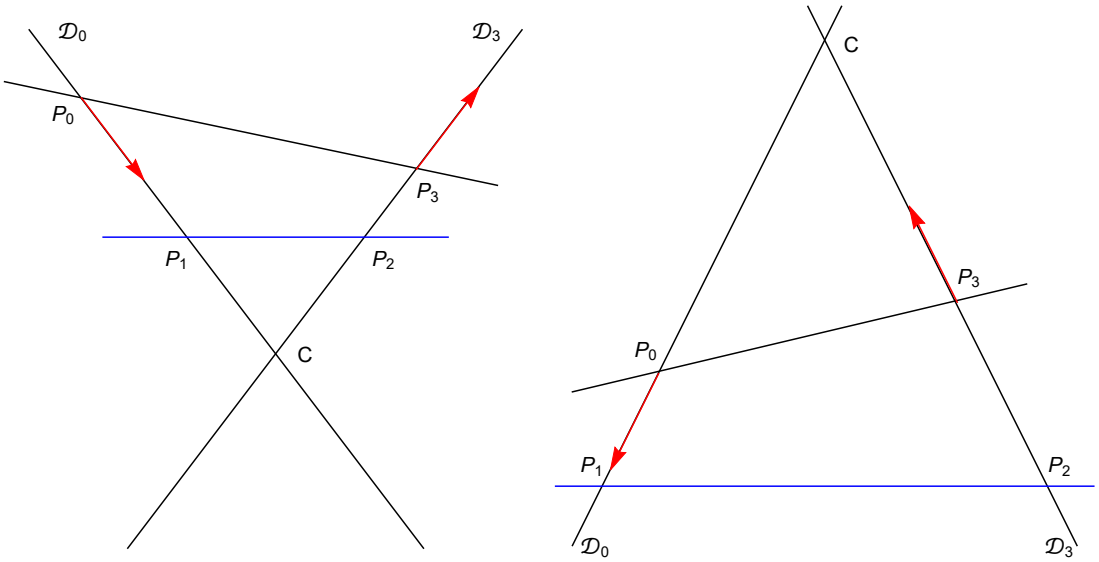

(a) Case 1: $0 \leq \theta_3 < \theta_0 + \pi$.

(b) Case 2: $\theta_0 + \pi < \theta_3 \leq \pi$.

Figure 9: Shape of the control polygon when the lines $\mathcal{D}_0$ and $\mathcal{D}_3$ instersect.

the different configurations of the control polygon.

Considering two points $\mathbf{A}$ and $\mathbf{B}$, we denote by $\overline{\mathbf{AB}}$ the algebraic measure from $\mathbf{A}$ to $\mathbf{B}$. Let $\mathcal{D}_0$ (resp. $\mathcal{D}_3$) be the line passing through $\mathbf{P}_0$ (resp. $\mathbf{P}_3$) with $\mathbf{t}_0$ (resp. $\mathbf{t}_3$) as the orientation vector. Firstly, we suppose the existence of the intersection point of $\mathcal{D}_0$ and $\mathcal{D}_3$, denoted by $\mathbf{C}$.

According to the initial constraints of the Hermite problem, the points $\mathbf{P}_1$ and $\mathbf{P}_2$ must be chosen such that $\overrightarrow{\mathbf{P_0P_1}}$ and $\mathbf{t}_0$ have the same orientation, and $\overrightarrow{\mathbf{P_3P_2}}$ and $\mathbf{t}_3$ are opposite vectors. The measures l_0 and l_2 are here defined algebraically, with $l_0 = \overline{\mathbf{P_0P_1}}$ and $l_2 = \overline{\mathbf{P_2P_3}}$, however these two values remain positive. Moreover, as $\theta_1 = \theta_2$ according to (2), the triangle $\mathbf{CP}_1\mathbf{P}_2$ is isosceles with apex $\mathbf{C}$. We therefore define the measures $a = \overline{\mathbf{CP}_0}$ and $b = \overline{\mathbf{CP}_3}$. These two values are constant with respect to α. As $\overline{\mathbf{CP_1}} = -\overline{\mathbf{CP_2}}$, we have $l_0 + a = l_2 - b$.

Moreover, the angles of $\mathbf{CP_0P_3}$ being fixed with respect to α, there exists a constant value c such that $l_1 = \pm c(l_0 + a)$. From relation (2), we deduce a new expression of K_α as a function of l_0, denoted $\widetilde{K}_\alpha$ and written as

$$\widetilde{K}_\alpha(l_0) = \frac{c^2(l_0 + a)^2}{l_0(l_0 + a + b)}.$$

In the considered domain, the function $\widetilde{K}_\alpha$ is an increasing and continuous bijection with respect to l_0. The proof, more tedious than difficult, needs to distinguish the cases $a < 0$ and $b > 0$ for $\theta_3 < \theta_0 + \pi$ (case a in Figure 9), and $a > 0$ and $b < 0$ for $\theta_3 > \theta_0 + \pi$ (case b in Figure 9). Moreover, the K_α form described in (1) is an increasing and continuous function of α (see Proposition 1). So $l_0 = \widetilde{K}_\alpha^{-1}(K_\alpha)$ is continuous and decreasing with respect to α. The property is also true for l_2, since $l_2 = l_0 + a + b$, the value $a + b$ being constant relative to K_α.

Proposition 4. *When $\varepsilon = 1$, $\theta_3 < \pi$ and $\mathcal{D}_0$ and $\mathcal{D}_3$ intersect, the lengths l_0 and l_2 continuously decrease as α increases.*

When $\mathcal{D}_0$ and $\mathcal{D}_3$ are parallel, we have $\theta_3 = \theta_0 + \pi$, as illustrated by Figure 10. Indeed, for $\theta_3 = \theta_0 + 2\pi$, Δ is always negative and the interpolation problem has no solution. Let $\mathbf{P'}_0$

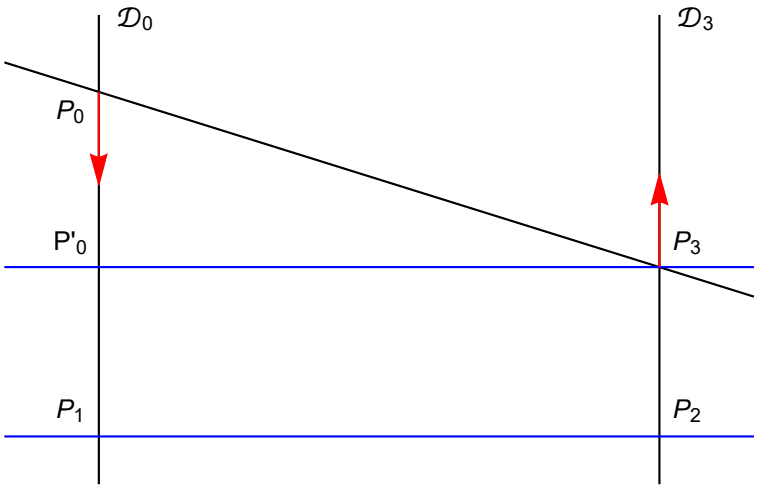

Figure 10: Shape of the control polygon when the lines $\mathcal{D}_0$ and $\mathcal{D}_3$ are parallel.

denote the projection of $\mathbf{P}_3$ onto $\mathcal{D}_0$, along the line $(\mathbf{P}_1\mathbf{P}_2)$ and we suppose that $\mathbf{P}_0\mathbf{P}_1 > \mathbf{P}_2\mathbf{P}_3$ (the other case being symmetrical, as before). Let a and c be the distances $\mathbf{P'}_0\mathbf{P}_0$ and $\mathbf{P'}_0\mathbf{P}_3$ respectively. Here again, these two values are independent of the choice of α. As $\theta_1 = \theta_2$, the quadrilateral $\mathbf{P'}_0\mathbf{P}_1\mathbf{P}_2\mathbf{P}_3$ is then a rectangle and we have $l_2 = l_0 - a$ and $l_1 = c$. So according to equation (2), $c^2 = K_\alpha l_0(l_0 - a)$. Hence, we define

$$\widetilde{K}_\alpha(l_0) = \frac{c^2}{l_0(l_0 - a)}.$$

Since $l_0 > a$, this function is obviously continuous and decreasing when $l_0 \in \mathbb{R}^+$. So, as for the intersecting case, we can establish the following result:

Proposition 5. *When $\varepsilon = 1$, $\theta_3 < \pi$ and $\mathcal{D}_0$ and $\mathcal{D}_3$ are parallel, the lengths l_0 and l_2 continuously decrease as α increases.*

Remark 3. *For $\varepsilon = 1$ and $\theta_3 < \pi$, the study points out that l_0 and l_2 also decrease as α increases. Though, for $\varepsilon = -1$ and $\theta_3 < \pi$, it can be proved that l_0 and l_2 are increasing functions with respect to α.*

5 Optimization process and numerical examples

As an example of a concrete use of the free parameter α in the Hermite interpolation described in this paper, we propose here an optimization process to determine its value required to satisfy an additional interpolation constraint. After determining the interval to which the α parameter should belong to get a solution, we infer the domain $\mathcal{P}$ where the extra interpolation point has to be to ensure the existence of a solution. The fitting process is developed and illustrated via some examples.

5.1 The domain $\mathcal{P}$

According to Section 3, the required conditions for the existence of a solution are $\Delta > 0$ and $G_\varepsilon > 0$. These constraints modify the initial interval $]0, 2\pi[$ of α. For $\varepsilon = 1$ and $\theta_3 < \pi$, we

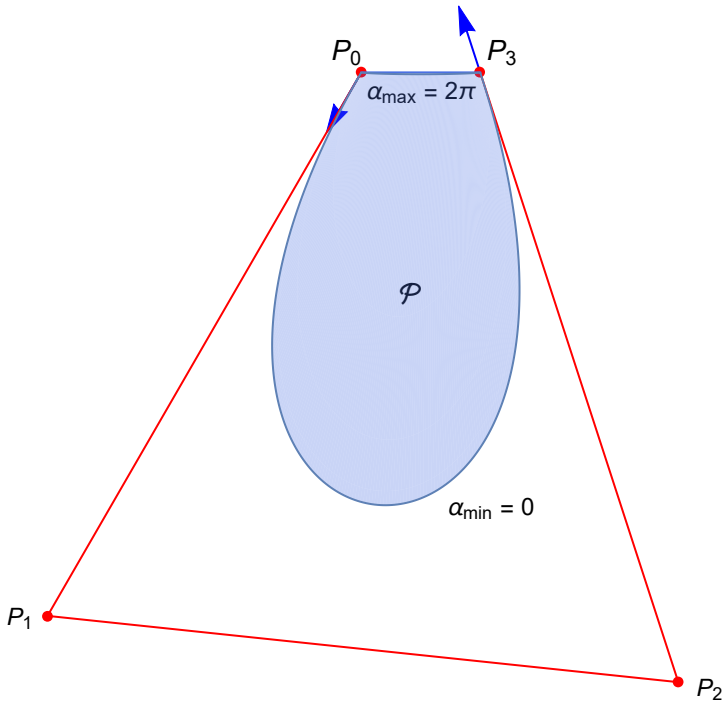

Figure 11: Domain $\mathcal{P}$ for $\theta_0 = -\frac{2\pi}{3}$, $\theta_3 = \frac{3\pi}{5}$ and $\alpha_{min} = 0$.

can determine α_{min} and α_{max}, depending on θ_0 and θ_3, such that the Hermite problem has a solution if and only if $\alpha \in]\alpha_{min}, \alpha_{max}[$.

On the studied domain, it can be easily proved that $\Delta > 0$. Therefore, the existence of a solution depends on the sign of G_+. Indeed, according to Proposition 3, we have $L_+ > 0$ if $G_+ > 0$ without any condition on α. Moreover, the domain Γ_+ is bounded by the condition $\theta_3 < \overline{\psi_1}(\theta_0)$. If $\theta_3 < \theta_0 + \dfrac{4\pi}{3}$ this inequality is always true and $\alpha_{min} = 0$ (as $K_\alpha \in]1, 4]$ from Proposition 1). Otherwise, it is equivalent to $K_\alpha > 2 + 2\cos(\theta_3 - \theta_0)$ and α_{min} is the value for which

$$K_\alpha = 2 + 2\cos(\theta_3 - \theta_0). \tag{15}$$

This equation being transcendental, no closed-form solution exists and a numerical approximation is therefore necessary. As there is no upper bound for Γ_+, we have evidently $\alpha_{max} = 2\pi$. The corresponding solution curve is then degenerated to the segment $[\mathbf{P}_0\mathbf{P}_3]$.

Properties 4 and 5 show that the lengths l_0 and l_2 continuously decrease as α increases. According to the variation diminishing property, the convex curve $\mathbf{r}_\alpha$ moves continuously from $\mathbf{r}_{\alpha_{min}}$ to $\mathbf{r}_{\alpha_{max}}$. The continuous curve $\mathbf{r}_\alpha$ then describes the area delimited by $\mathbf{r}_{\alpha_{min}}$ and $[\mathbf{P}_0\mathbf{P}_3]$, which is then the domain $\mathcal{P}$ we are looking for. So, for any point $\mathbf{D}$ in $\mathcal{P}$, there exists $\alpha_* \in]\alpha_{min}, \alpha_{max}[$ and $t_D \in [0, \alpha_*]$ such that $\mathbf{r}_{\alpha_*}(t_D) = \mathbf{D}$. Figure 11 illustrates the domain $\mathcal{P}$ for $\theta_0 = -\frac{2\pi}{3}$ and $\theta_3 = \frac{3\pi}{5}$ for which $\alpha_{min} = 0$.

Remark 4. *When $\theta_3 > \theta_0 + \dfrac{4\pi}{3}$ and α_{min} is a solution of (15), we have $G_+ = 0$ implying that the length $l_0 = \dfrac{\|\mathbf{P}_3 - \mathbf{P}_0\|}{G_+}$ is theoretically infinite. Practically, even though the used value is an approximation, l_0 still increases dramatically with the accuracy of α_{min}. Even if it can be seen as an advantage since it involves a very large $\mathcal{P}$ domain, it can lead to serious numerical*

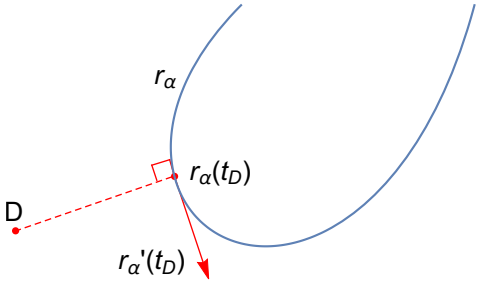

Figure 12: Orthogonal projection.

instabilities when verifying the belonging of $\mathbf{D}$ *to* $\mathcal{P}$ *and determining* α_**. It is rather preferable to choose a value slightly greater than the solution of* (15) *for* α_{min}*.*

5.2 The optimization process

First, the point $\mathbf{D}$ must be reachable (otherwise, the optimization process would obviously be useless). The belonging of $\mathbf{D}$ to $\mathcal{P}$ can be verified with a ray-tracing method (cf. Shimrat [10] for more details about the process), which is applied to the polygon defined by $[\mathbf{P_0P_3}]$ and a discretization of $\mathbf{r}_{\alpha_{min}}$.

Satisfying the interpolation constraint consists of minimizing the fitting error defined by $E(\alpha) = \|\mathbf{D} - \mathbf{r}_\alpha(t_D)\|^2$ where $t_D \in [0, \alpha]$ is the parameter related to the closest orthogonal projection of $\mathbf{D}$ onto $\mathbf{r}_\alpha$, as shown in Figure 12. In other words, its value t_D is obtained by determining the solution of

$$\mathbf{r}'_\alpha(t).(\mathbf{D} - \mathbf{r}_\alpha(t)) = 0 \tag{16}$$

that minimizes the distance between $\mathbf{D}$ and $\mathbf{r}_\alpha(t)$.

Equation (16) being transcendental, a numerical approximation is necessary to get t_D for a given value of α. As described by Piegl and Tiller in [8], an iterative Newton-Raphson-based approach is used to calculate the error $E(\alpha)$.

A dichotomy-based process is defined to obtain α_*, the value of α for which the minimum of $E(\alpha)$ is approximated. Each iteration, whose rank is denoted by k, can be summed up in 4 steps:

1. Compute the current parameter denoted α_k, middle of the domain $[\alpha_{min}, \alpha_{max}]$.
2. Update the control points with the α_k parameter.
3. Discretize $\mathbf{r}_{\alpha_k}$.
4. Update α_{min} (resp. α_{max}) according to the belonging (resp. non-belonging) of the point $\mathbf{D}$ in the hull of $\mathbf{r}_{\alpha_k}$ with the ray-tracing method.

The process is stopped when $E(\alpha_k) < \eta$, with η a given accuracy. The reader can refer to Appendix A for further details about the steps listed above.

5.3 Numerical examples

In this part, we propose two numerical examples to illustrate the process developed in Section 5.2, namely the construction of a quarter circle followed by a more general fitting case.

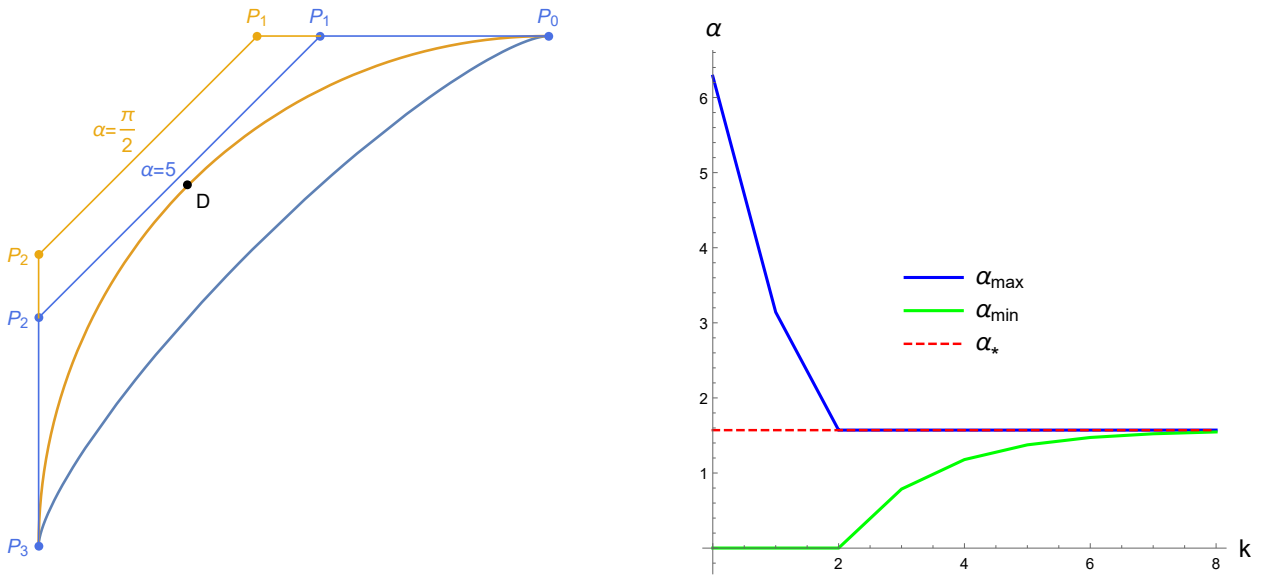

(a) Two ATPH curves: $\mathbf{r}_5$ and the quarter circle $\mathbf{r}_{\frac{\pi}{2}}$.

(b) Evolution of α_{min} and α_{max} towards $\alpha_* = \frac{\pi}{2}$.

Figure 13: Construction and convergence for the quarter circle.

The construction of a quarter circle, for which the value of α_* is easy to determine exactly, allows us to illustrate the convergence of the process to the solution. For this purpose, we choose $\mathbf{P_0} = (0, 1)$, $\mathbf{P_3} = (-1, 0)$, $\theta_0 = -\frac{\pi}{4}$, $\theta_3 = \frac{\pi}{4}$ and $\mathbf{D} = \left(-\frac{\sqrt{2}}{2}, \frac{\sqrt{2}}{2}\right)$ the point to interpolate.

According to Proposition 5 in [4], the ATPH is a circle arc if and only if $l_0 = l_2$ and $\theta_1 = \theta_2 = \frac{\alpha}{2} - \pi$. In other words, we have $-\theta_0 = \theta_3 = \frac{\alpha}{2}$ where α has to be chosen as the arc length of the curve (here $\alpha = \frac{\pi}{2}$) as put forward in Figure 13a. Figure 13b shows the fast convergence of α_{min} and α_{max} to the expected value $\alpha_* = \frac{\pi}{2}$.

In the second example, we consider $\theta_0 = -1$, $\theta_3 = 0.99\ \pi$ and $\mathbf{D}$ near the borderline of the domain $\mathcal{P}$. Figure 14 illustrates the iterative fitting process. The eight ATPH in blue (of which only the first five are indexed for the sake of clarity) are intermediate curves leading to $\mathbf{r}_{\alpha_*}$ in orange, where $\alpha_* = 3.09$. The solution $\mathbf{r}_{\alpha_*}$ is pointed out with its associated control polygon.

6 Conclusion

Here, we have studied the construction process of a Hermite interpolation within the framework of the cubic ATPH. The domain Γ in which solutions exist has been rigorously described. Through the presence of the α parameter, the solution of the Hermite problem provided by ATPH curves is not unique. The analysis carried out between the parameter α and the control polygon allows us to understand its influence on the curve. This degree of freedom can be taken into account to solve additional problems. We have proposed an example through a fitting process.

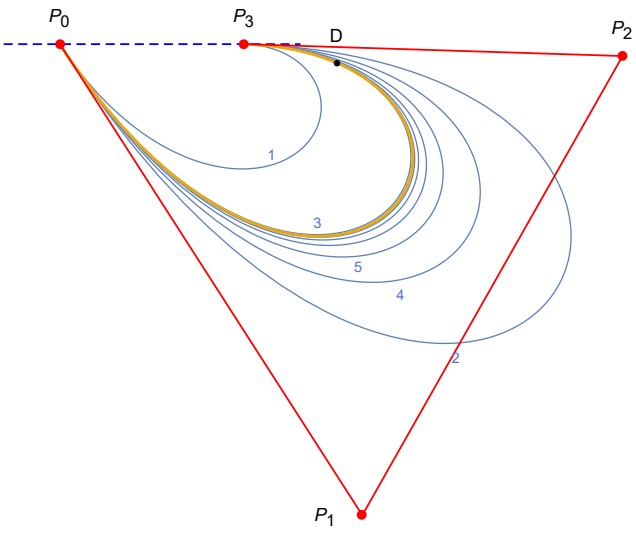

Figure 14: Iterative fitting process from intermediate curves in blue to $\mathbf{r}_{\alpha_*}$ in orange.

References

[1] M. Byrtus and B. Bastl. G1 Hermite interpolation by PH cubics revisited. *Computer Aided Geometric Design*, 27(8):622–630, 2010. Advances in Applied Geometry.

[2] J.M. Carnicer and J.M. Peña. Totally positive bases for shape preserving curve design and optimality of b-splines. *Computer Aided Geometric Design*, 11(6):633–654, 1994.

[3] I. Cattiaux. Normalized C-Basis and C-Curves. *Wolfram Demonstration Project*, March 2015.

[4] I. Cattiaux-Huillard and L. Saini. Characterization and extensive study of cubic and quintic algebraic trigonometric planar PH curves. *Advances in Computational Mathematics*, 46(2):28, 2020.

[5] R. T. Farouki and T. Sakkalis. Pythagorean Hodographs. *IBM J. Res. Develop.*, 34:736–752, 1990.

[6] E. Mainar, J. M. Peña, and J. Sánchez-Reyes. Shape preserving alternatives to the rational Bézier model. *Computer Aided Geometric Design*, 18(1):37–60, February 2001.

[7] D.S. Meek and D.J. Walton. Geometric Hermite interpolation with Tschirnhausen cubics. *Journal of Computational and Applied Mathematics*, 81(2):299–309, 1997.

[8] L. Piegl and W. Tiller. *The NURBS book (2nd ed.)*. Springer-Verlag New York, Inc., 1997.

[9] L. Romani, L. Saini, and G. Albrecht. Algebraic-Trigonometric Pythagorean-Hodograph curves and their use for Hermite interpolation. *Advances in Computational Mathematics*, 40(5-6):977–1010, 2014.

[10] M. Shimrat. Algorithm 112: Position of Point Relative to Polygon. *Communications of the ACM*, 5(8):434, August 1962.

[11] J. Zhang. C-curves: An extension of cubic curves. *Computer Aided Geometric Design*, 13(3):199–217, 1996.

A Algorithm of the optimization process

Algorithm 1: Optimization with respect to α

Input: Point $\mathbf{D}$ to fit, computational accuracy parameter η
Output: The optimized value of α

$\alpha_{max} \leftarrow 2\pi$
$\alpha_{min} \leftarrow 0$

if $\theta_3 > \theta_0 + \frac{4}{3}\pi$ **then**
    $\alpha_{min} \leftarrow \arg\min_{\alpha} |K_\alpha - 2 - 2\cos(\theta_3 - \theta_0)|$
    // $\arg\min$ stands for argument of the minimum, i.e. the elements of the domain at which the function value is minimized
end

// Loop to reduce iteratively the research interval
$k \leftarrow 0$
$d_{err} \leftarrow E\left(\frac{\alpha_{min} + \alpha_{max}}{2}\right)$

while $d_{err} > \eta$ **do**
    $\alpha_k \leftarrow \frac{\alpha_{min} + \alpha_{max}}{2}$
    Update the control points relating to $\mathbf{r}_{\alpha_k}$
    Compute hull of $\mathbf{r}_{\alpha_k}$
    if $\boldsymbol{D} \in$ *hull of* $\mathbf{r}_{\alpha_k}$ **then**
        $\alpha_{min} \leftarrow \alpha_k$
    else
        $\alpha_{max} \leftarrow \alpha_k$
    end
    $d_{err} \leftarrow E(\alpha_k)$
    $k \leftarrow k + 1$
end

return α_k